Polymer Journal (2014) 46, 598–608

www.nature.com/pj

ORIGINAL ARTICLE

Cross-linking and damping properties of poly(caprolactone-co-glycidyl methacrylate)

Hang Shen[1,2,3], Jianding Chen[4] and Mohamed Taha[1,2,3]

Poly(caprolactone-co-glycidyl methacrylate), p(CL-co-GMA), was prepared by ring-opening copolymerization in a one-step solvent-free process. 1,5,7-Triazabicyclo[4,4,0]dec-5-ene, stannous octoate and 4-hydroxybenzenesulfonic acid were tested separately as catalysts, and the copolymerization parameters were optimized. Analyses of the obtained copolymers, principally by matrix-assisted laser desorption/ionization–time of flight, confirmed the copolymerization, as macrocycles and linear chains were detected. Networks of p(CL-co-GMA) were prepared using 2-hydroxyethyl methacrylate and/or multi-mercapto coupling agents. Thermomechanical analyses of the obtained networks were conducted. Of particular importance, damping over a wide range of temperatures was observed for some materials.
Polymer Journal (2014) **46,** 598–608; doi:10.1038/pj.2014.29; published online 4 June 2014

Keywords: acrylated polycaprolactone; damping; glycidyl methacrylate; network; poly(hydroxyethyl methacrylate); ring-opening copolymerization; thiol–ene reaction

INTRODUCTION

Polymers can be designed with particular damping properties, and these polymers can absorb shocks and transform mechanical energy into heat, especially in their relaxation region from the glassy to elastic rubbery states.[1–3] However, for most (co)polymers or their blends, the temperature region of damping is relatively narrow.[4–6] Therefore, polymer hybrids and interpenetrating networks have been designed and used as damping materials.[1–3]

Poly(ε-caprolactone), PCL, is an important synthetic biodegradable polymer.[7–9] It can be processed using classical polymer processing techniques[7–12] and has been used for a variety of applications, such as sutures, bone fixation and drug-release carriers in the medical field.[13–16] If PCL chains are interconnected with other polymer segments or a multifunctional coupling agent, networks with wide relaxation areas can be obtained. These bio-based networks are expected to have damping properties over a wide temperature range. The elaboration of such materials will be considered in this study.

However, as a linear polyester, PCL lacks pendant functional groups that could be interconnected by well-controlled methods, which greatly limits its use in network elaboration. Thus, different strategies have been reported to endow PCL with reactive pendant functional groups. When activated by ultraviolet (UV) or plasma irradiation in oxidant environments (O_2 or H_2O_2), PCL can generate radical centers that can lead to cross-linking by combination.[17,18] Using another approach, linear or branched PCL was prepared using a chain termination agent bearing a reactive functional group, such as a double bond[19,20] or furan.[19,20] In other previous studies, caprolactone derivatives bearing double bonds were synthesized and copolymerized with caprolactone. During this process, PCL with reactive centers was dispersed randomly along the chain;[21,22] these PCL derivatives can form networks by homo- or copolymerization.

Although the last method is highly efficient, modified ε-caprolactone is not commercially available, and its large-scale preparation is relatively complicated. In this study, rather than using functionalized ε-caprolactone, a novel and simple method is proposed for the synthesis of PCL with double bonds dispersed randomly along the chain. The direct ring-opening copolymerization of ε-caprolactone and GMA is evaluated and optimized. The obtained methacrylated PCL is copolymerized with 2-hydroxyethyl methacrylate (HEMA) or coupled with multi-mercapto reagents, leading to networks with different structures. The interconnection of PCL chains by poly(HEMA) (pHEMA) segments with varying chain lengths leads to networks with wide relaxation temperature regions. Nevertheless, in the literature, thermomechanical analysis has not been developed, particularly with respect to the damping properties of PCL-based networks. In this study, the damping properties of the networks are analyzed in relation to their structures.

MATERIALS AND METHODS

Materials

HEMA was purchased from Röhm GmbH (RÖHM S.A.R.L., St. Maximin, France). Hydroquinone (99%), ε-caprolactone (>99%), benzyl alcohol

[1]Université de Lyon, Saint-Etienne, France; [2]CNRS, UMR 5223, Ingénierie des Matériaux Polymères, Saint-Etienne, France; [3]Université de Saint-Etienne, Jean Monnet, Saint-Etienne, France and [4]Laboratory of Advanced Materials Processing, East China University of Science and Technology, Shanghai, China
Correspondence: Professor M Taha, Ingénierie des Matériaux Polymères, Universite Jean Monnet, IMP-UJM, Faculté de Sciences et Techniques, 23 rue du Dr Paul Michelon, 42023 Saint-Etienne Cedex 2, France.
E-mail: Mohamed.Taha@univ-st-etienne.fr
Received 4 February 2014; revised 13 March 2014; accepted 18 March 2014; published online 4 June 2014

(BzOH), 1,5,7-triazabicyclo[4.4.0]dec-5-ene (TBD), tin(II) bis(2-ethylhexanoate) [$Sn(Oct)_2$], 4-hydroxybenzenesulfonic acid solution (65%, in H_2O) (4-HBSA), trimethylolpropane tris(3-mercaptopropionate) and GMA (97%) were purchased from SIGMA-ALDRICH (Sigma-Aldrich Chimie S.a.r.l., Lyon, France).

The photoinitiator was composed of the following reagents: 60 wt% CN381 from Arkema-Sartomer (Arkema, Colombes, France); 20 wt% benzophenone (99%) and 20 wt% 2,2-diethoxyacetophenone from SIGMA-ALDRICH. ε-Caprolactone and HEMA were distilled before use. All other reagents were used as received.

Instrumentation

Infrared spectroscopy. Fourier transform infrared spectroscopy (FTIR) absorption spectra of the polymer were recorded on a Nicolet Nexus spectrometer (Nicolet Nexus spectrometer, Thermo Scientific, Illkirch, France) (700–3500 cm^{-1}) using the attenuated total reflectance technique.

Nuclear magnetic resonance analysis. Nuclear magnetic resonance (NMR) analyses were performed with a BRUKER Advance III spectrometer (Bruker, BioSpin S.A.S, Wissembourg, France) operating at 400 MHz for ^1H NMR analyses and at 100.6 MHz for ^{13}C NMR analyses. The analyses were performed with 10 mm diameter tubes containing ~400 mg of polymer in 0.6 ml of chloroform-D, with tetramethylsilane as the internal reference at 0 p.p.m.

Matrix-assisted laser desorption/ionization–time of flight spectroscopy. Matrix-assisted laser desorption/ionization–time of flight (MALDI–TOF) analysis was performed on a BRUKER Daltonics Ultraflex III. The polymer samples were dissolved in dimethylsulphoxide. The cationization agent was sodium iodide dissolved in acetone at a concentration of 10 mg ml^{-1}. The matrix was dithranol dissolved in dimethylsulphoxide at a concentration of 10 mg ml^{-1}. Solutions of matrix, salt and polymer were mixed in a volume ratio of 10/1/1.

Differential scanning calorimetry. Differential scanning calorimetry measurements were performed using a Q10 calorimeter from TA Instruments (Guyancourt, France). Samples were transferred to and sealed in hermetic pans and then analyzed from −80 to 150 °C with a cooling/heating rate of 10 °C min^{-1}. The glass transition temperatures were evaluated from the data recorded during heating by identifying the inflection points. Each sample underwent two heating–cooling cycles.

Size exclusion chromatography. Size exclusion chromatography was conducted using a system equipped with refractive index (Waters 2414, Waters SAS, Guyancourt, France), viscosimeter (Wyatt ViscoStar, Wyatt Technology, Toulouse, France) and light scattering (Wyatt MiniDawnTreos, Wyatt Technology) detectors. Three columns, HR 0.5, HR1 and HR3, from Waters were used. The eluent was tetrahydrofuran with a flow rate of 1 ml min^{-1}, and the elution temperature was 35 °C. The copolymer molecular weights were determined using a calibration curve established from a set of polystyrene standards of different molecular weights ranging from 500 to 700 000.

Dynamic mechanical analysis. Rheological measurements in the solid state were performed with a Rheometric Scientific ARES N2, Rheometric Scientific, Piscataway, NJ, USA. Specimens prepared with a predetermined shape (30 mm × 2 mm × 10 mm) were subjected to sinusoidal microstrain with fixed autotension at a constant frequency of 1.0 rad s^{-1}. Dynamic temperature sweep tests were chosen with strain amplitudes of 0.01% to maintain the measured torque at a sufficient level, and a heating rate of 3 °C min^{-1} from −85 to 100 °C was used.

EXPERIMENTAL

Synthesis

Copolymerization between CL and GMA was accomplished in a 250-ml glass reactor (62 mm diameter) with a three-neck steel cover. A steel anchor stirrer operating with a RW 28 W motor, IKA (Staufen, Germany) motor at 60 r.p.m., condenser and T-type thermocouple probe were fixed to the cover. Nitrogen flow, previously dried in a silica column, eliminated air from the reactor. The reactor was heated by an IKA HBR4 bath with silicone oil.

Copolymerization of CL and GMA

CL, BzOH and hydroquinone were mixed and introduced to the reactor at 110 °C. GMA was introduced into the reactor 10 min later. When the system was completely homogeneous and thermally stabilized, TBD was introduced, and the reaction was maintained for 45 to 180 min. The product was dissolved in chloroform, precipitated in cold ethyl ether, filtered and dried under vacuum at room temperature for 48 h and then stored at −20 °C.

Radical polymerization of p(CL-co-GMA) and HEMA by photoirradiation

The copolymer of CL and GMA was dissolved simultaneously in HEMA and trimethylolpropane tris(3-mercaptopropionate) in different mass ratios by oscillation at room temperature for 3 min. The photoinitiator was then added and mixed. The mixture was placed in an ultrasonic oscillator to remove air bubbles before curing. To initiate UV irradiation, reagent mixtures were placed in Teflon molds (40 mm × 10 mm × 0.1 mm) and cured in air by a fluorescent lamp, JAD STS-350 (Boyu, Guangdong, China), equipped with 8 W × 3 fluorescent tubes providing $\lambda = 250$ nm UV light. The mixtures were exposed at a distance of 3 cm from the lamps for 24 h. After curing, the sample bars were collected for mechanical analyses.

RESULTS AND DISCUSSION

GMA can polymerize or copolymerize by ring opening of the epoxy group. In this case, the methacrylate functional group remains available for further modification.[23–26] Bednarek and Kubisa[27] copolymerized CL with ethylene oxide to prepare hydroxy telechelic PCL. Uenishi *et al.* also reported the copolymerization of cyclic ester and glycidyl phenyl ether.[28] On the basis of these studies, the copolymerization of GMA and CL appears to be reasonable. In this study, this copolymerization is verified.

Synthesis and characterization of p(CL-co-GMA) copolymer

P(CL-co-GMA) copolymers were prepared through the ring-opening copolymerization of caprolactone and the epoxy functional group of GMA. In this study, TBD, $Sn(Oct)_2$ and 4-HBSA were separately used as catalysts. No solvents were used in these syntheses. The obtained copolymers are expected to contain unreacted pendant double bonds on the backbone, as illustrated in Scheme 1.

Qualitative analysis of the obtained copolymers. The obtained products were analyzed by ^{13}C NMR. Figure 1 shows a representative ^{13}C

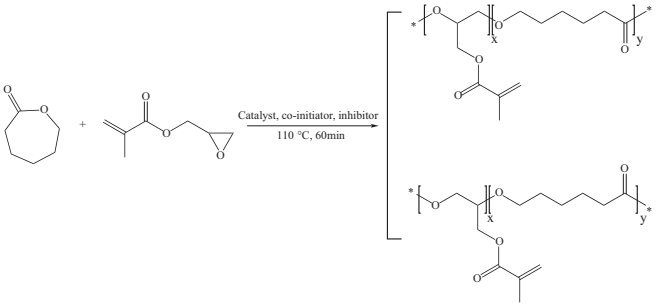

Scheme 1 Ring-opening copolymerization of caprolactone and glycidyl methacrylate.

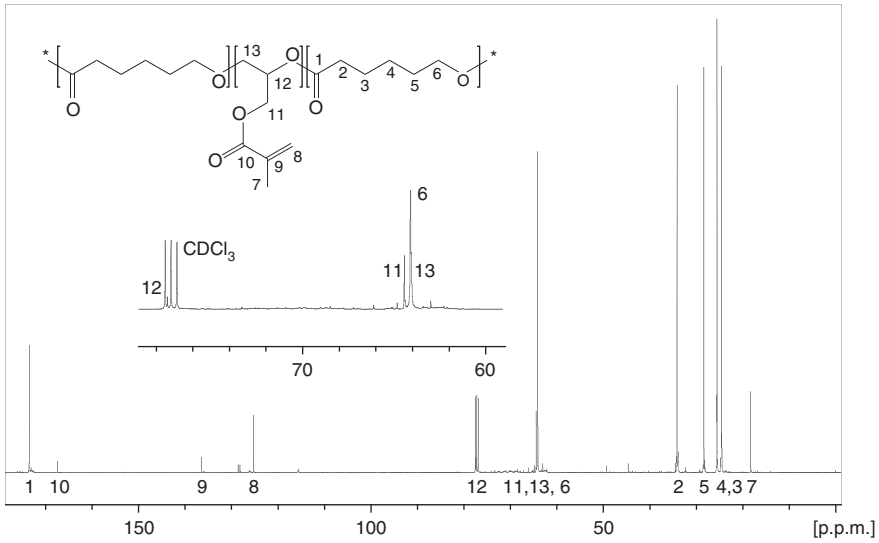

Figure 1 ^{13}C NMR spectrum of p(glycidyl methacrylate-co-caprolactone) in $CDCl_3$. The sample was synthesized with [CL]/[GMA] = 5 and [CL]/[TBD]/[benzyl alcohol]/[hydroquinone] = 100/1/1/1 at 110 °C for 60 min. CL, caprolactone; GMA, glycidyl methacrylate; NMR, nuclear magnetic resonance; TBD, 1,5,7-triazabicyclo[4.4.0]dec-5-ene.

NMR spectrum of a non-purified copolymer. The resonances attributed to the different carbons of the copolymer are shown in Figure 1. Under the copolymerization parameters used, there is no residual caprolactone monomer in the system. Carbons on the caprolactone repeat unit can easily be located, labeled from 1 to 6, as well as GMA repeat unit carbons, labeled from 7 to 13 in the spectrum. The presence of a few unreacted epoxy cycles is detected by the persistence of carbons from unreacted epoxy rings at 44.6 and 49.4 p.p.m.

To confirm that CL and GMA copolymerized by ring-opening polymerization, matrix-assisted laser desorption/ionization–time of flight analyses of the obtained products were performed. Figure 2a provides an overview of the obtained polymers with molecular weights ranging from 600 to 3000, which is in accordance with the below results from size exclusion chromatography. From Figure 2b, several series of macromolecules containing different GMA units can be identified, showing that the composition of the obtained product is in fact not uniform. As expected, all the series primarily contain CL repeat units, as indicated by the molecular weight increment of 114.06 g mol^{-1}. The series containing two, one and zero GMA units are those with the highest intensities. All easily detectable series contain only CL and GMA units, suggesting that they are macrocycles. Linear chains with lower intensities were detected; these chains also contain GMA repeat units.

From these analyses, it can be concluded that a copolymer containing CL and GMA repeat units can be obtained through the ring-opening copolymerization of GMA and CL. The product also contains PCL as macro rings, but the homopolymerization of GMA was not observed from qualitative analysis.[29]

Quantitative analysis of the obtained polymers. On the basis of qualitative results presented above, quantitative analyses were also conducted. The expected structure of a p(CL-co-GMA) prepared by ring opening polymerization is shown in Scheme 1. The obtained polymer was purified to remove the unreacted monomer, catalyst and initiator and was analyzed by ^1H NMR to evaluate the structure of the polymer, as shown in Figure 3.

Protons from GMA and caprolactone repeat units are clearly observed in the ^1H NMR spectra. The epoxy ring reacted (with no epoxy ring protons at 2.6, 2.8 and 3.2 p.p.m.), whereas the double bond remained in the system, with proton chemical shifts at 5.6 and 6.1 p.p.m. Moreover, there is no residual caprolactone monomer. Proton A′ is the end-chain ε-proton of the caprolactone repeat unit. The triplet A, representing the caprolactone ε-methylene proton, splits into two parts, likely caused by CL connected to different repeat units, CL or GMA. This result again proves the copolymerization of CL and GMA because the integral ratio of these two peaks is close to the feeding ratio and the sum of these two peaks is always equal to the integral of α-methylene protons from caprolactone repeat units for all samples with different monomer feeding rates. Owing to the epoxy ring-opening mechanism, there may be two types of chain propagation: the nucleophile attacks either the least substituted carbon, in accordance with standard SN_2 nucleophilic addition, or the most substituted carbon by steric effects and carbocationic stability,[30] as shown in Scheme 1. For the obtained products, the backbone protons (I, I′, J, J′) generated by the epoxy ring cannot be quantified because they are overlapped by protons A and A′ and also overlap each other at ~3.7–4.5 p.p.m. Protons E and F correspond to the α-methylene group from the CL repeat unit and the methyl group from the GMA repeat unit, respectively.

Consequently, the average ratio of these two repeat units can be calculated by the integration ratio:

$$r = 3E/2F,$$

whereas the average functionality f can be obtained using the M_n from size exclusion chromatography:

$$f = M_n/(114.04 \times r + 142.15).$$

Furthermore, the conversion of GMA into repeat units can also be calculated by:

$$p = ([GMA]/[CL])/([GMA]_0/[CL]_0),$$

where [GMA] and $[GMA]_0$ correspond to the GMA contents of the obtained polymer and in the formulae; CL conversion is considered to be 100%. Following the equations above, the quantitative analyses of the samples synthesized with different parameters are listed in Table 1.

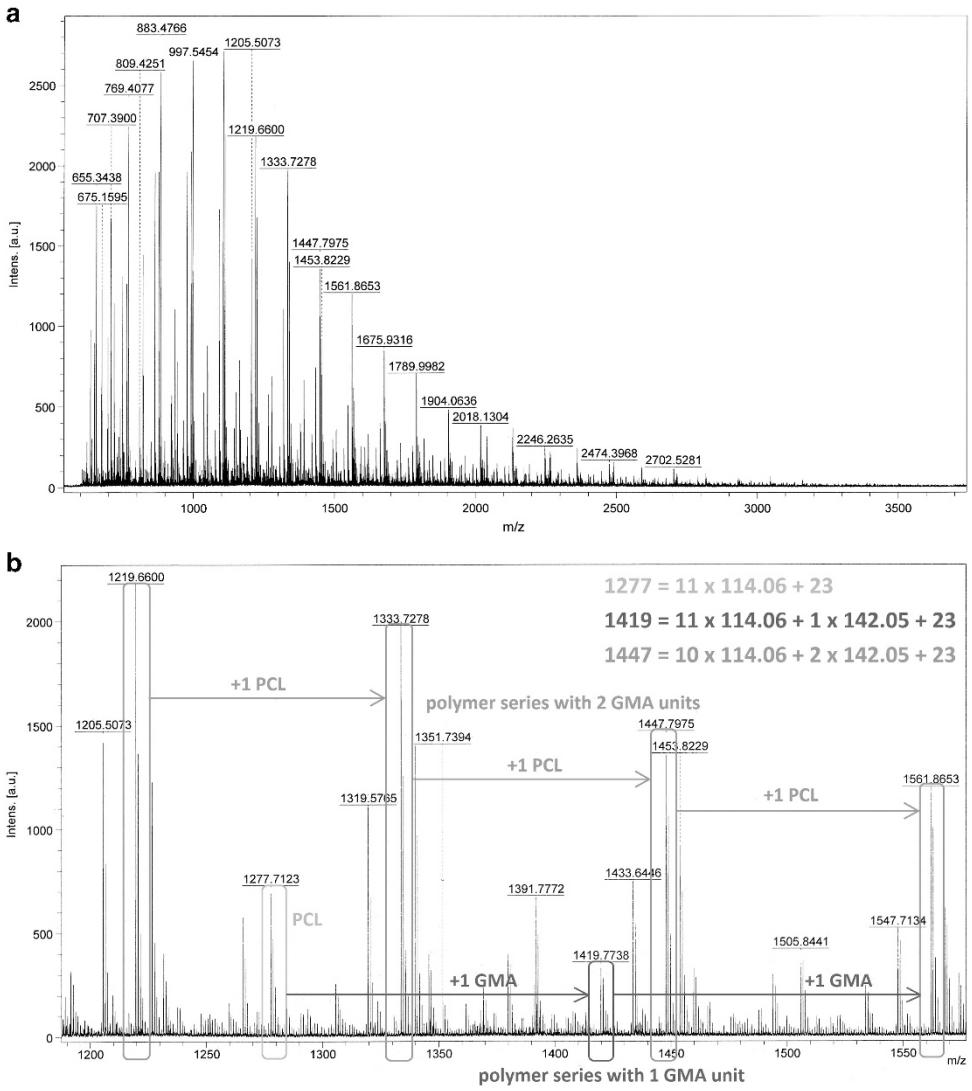

Figure 2 (**a**) MALDI–TOF spectrum of p(glycidyl methacrylate-co-caprolactone) with m/z from 600 to 2500. The sample was synthesized with [CL]/[GMA] = 5 and [CL]/[TBD]/[benzyl alcohol]/[hydroquinone] = 100/1/1/1 at 110 °C for 60 min. (**b**) MALDI–TOF spectrum of p(glycidyl methacrylate-co-caprolactone) with m/z from 1200 to 1600. The sample was synthesized with [CL]/[GMA] = 5 and [CL]/[TBD]/[benzyl alcohol]/[hydroquinone] = 100/1/1/1 at 110 °C for 60 min. CL, caprolactone; GMA, glycidyl methacrylate; MALDI–TOF, matrix-assisted laser desorption/ionization–time of flight; TBD, 1,5,7-triazabicyclo[4.4.0]dec-5-ene. A full color version of this figure is available at *Polymer Journal* online.

These pre-polymers were designed to have relatively low molecular weights, so they remain readily soluble in HEMA.

Synthesis optimization. Different parameters can be used to investigate and optimize the copolymerization, including the type and amount of initiator, the ratio of initiator to co-initiators and the monomer feeding ratios. The obtained polymers were quantified to characterize the monomer conversion and copolymer molar mass and average functionalities, through which the optimal synthesis parameters were obtained, as described below.

Catalyst efficiency. In this study, $Sn(Oct)_2$, TBD and 4-HBSA were used as catalysts. The reactions were monitored by Fourier transform infrared spectroscopy. GMA conversion was evaluated by epoxy ring absorption in Figure 4 and NMR analysis.

From the IR spectra, in which carbonyl absorption ($1726\,cm^{-1}$) is a constant peak, the epoxy ring was almost consumed in TBD and $Sn(Oct)_2$ systems, whereas GMA monomer remains in the 4-HBSA system, as illustrated by the change in epoxy ring absorption (906 and $1250\,cm^{-1}$, γ_{c-o}).[31–33] However, a decrease in double-bond absorption at $1635\,cm^{-1}$ [34] in the $Sn(Oct)_2$ system indicates consumption of double bonds. This result corresponds with the data obtained from the NMR analysis, as shown in Table 2.

The conversion of CL and GMA to repeat units was also investigated by ^1H NMR to obtain precise results. With 4-HBSA as the catalyst, a considerable amount of CL remained unconsumed after 60 min; gelation also occurred in the system, whereas many double bonds were lost in the $Sn(Oct)_2$-catalyzed system. By contrast, TBD showed high GMA conversion, and no double bonds were lost during copolymerization; therefore, TBD was chosen as the catalyst in this study.

Effects of TBD/BzOH amount and ratios on GMA/CL copolymerization. When used as the catalyst, the amount of TBD greatly affects the reaction speed of polymerization from seconds to several hours. Six conversion-time kinetic curves of GMA and CL were obtained by

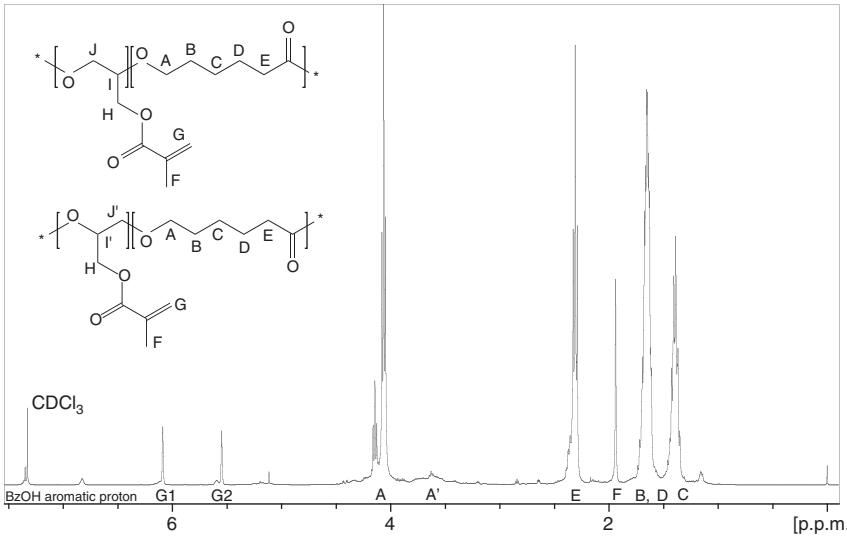

Figure 3 ^{1}H NMR spectrum of purified p(glycidyl methacrylate-co-caprolactone) in $CDCl_3$. The sample was synthesized with [CL]/[GMA] = 5 and [CL]/[TBD]/[benzyl alcohol]/[hydroquinone] = 100/1/1/1 at 110 °C for 60 min. CL, caprolactone; GMA, glycidyl methacrylate; NMR, nuclear magnetic resonance; PCL, poly(ε-CL); TBD, 1,5,7-triazabicyclo[4.4.0]dec-5-ene.

Table 1 Caprolactone and glycidyl methacrylate copolymerization at 110 °C for 60 min

Sample	*Feeding ratio [CL]:[GMA]*	*Repeat unit ratio [CL]:[GMA]*	*[TBD]:[BzOH] amount, mol%:mol%*	*GMA (as repeat unit) %*	*Molar mass by SEC, MW/M_n/MWD*	*Average functionality*
Run 1[a]	1:1	—	1:1	—	—	—
Run 2	2.5:1	4.4:1	1:1	56.8	4550/2430/1.87	3.2
Run 3	5:1	6.5:1	1:1	76.95	7660/4100/1.87	4.6
Run 4	10:1	14:1	1:1	70.56	10 860/5790/1.79	3.1
Run 5	20:1	43:1	1:1	47.21	11 950/6100/1.96	1.2
Run 6	5:1	7.5:1	0.5:1	35.6	2700/1330/2.03	1.3
Run 7[a]	5:1	10:1	0.2:1	—	—	/
Run 8	5:1	6.5:1	1:0.5	61.69	6730/3700/1.82	4.2
Run 9	5:1	6.3:1	1:2	67.21	4640/2540/1.82	2.9
Run 10	5:1	6.8:1	0.75:1.5	45.15	6310/3190/1.97	3.5

Abbreviations: BzOH, benzyl alcohol; CL, caprolactone; GMA, glycidyl methacrylate; MW, molecular weight; MWD, molecular weight distribution; SEC, size exclusion chromatography; TBD, 1,5,7-triazabicyclo[4.4.0]dec-5-ene.
[a]For the insolubility (Run 1) and uncompleted reaction (Run 7), the SEC analyses of these two products.

varying the catalyst concentration at 110 °C. The conversion of GMA was calculated by ^{1}H NMR spectroscopy using the integral ratio between double-bond proton resonances from the monomer and repeat unit at 6.10 and 6.16 p.p.m., respectively. For CL, the conversion can be calculated by CL α-methylene proton chemical shifts for the monomer and repeat unit, located at 2.0 and 2.4 p.p.m., respectively. The results are listed in Table 1 (Run 3 and 6–10) and illustrated in Figures 5 and 6.

As shown in Figures 5 and 6, the amount of TBD greatly affects the reaction rate and conversion of GMA. With higher TBD content, 80 mol% of the GMA monomer was consumed within 1 h compared with those with only 0.2 mol% TBD, for which the GMA conversion was no more than 50% even after 2.5 h. However, as a strong guanidine base that can complex the inhibitor (hydroquinone) and induce the cationic polymerization of double bonds, an excess of TBD (> 2 mol% of CL) will lead to uncontrollable cross-linking within seconds.

BzOH reacts with the intermediate generated from the nucleophilic reaction of TBD with lactone.[35] Thus, the concentration of BzOH affects the consumption of GMA; however, its effect is not as obvious as that of the catalyst in this study. The effect of the [CL]/[BzOH] mole ratio on the molar mass of the products is shown in Table 1 (Run 8–10). For the copolymerization of CL, the monomer consumption rate depends mainly on the amount of catalyst in the system. The copolymerization proceeds efficiently when the amount of catalyst is higher than 0.5 mol% CL, on which the reaction of CL is completed in 60 min. Although the conversion of GMA remains stable after the consumption of CL, the homopolymerization of GMA will not occur when using TBD as catalyst, which is proven again by individual experiments mixing TBD, hydroquinone and GMA at 110 °C for 1.5 h

Effect of monomer feeding ratio [GMA]/[CL] on copolymerization. To increase the functionality of the copolymer and to endow more pendant double bonds on the chains, the [GMA]/[CL] feeding ratio was altered to investigate its effects on the polymer content. The obtained polymer was characterized by size exclusion chromatography and ^{1}H NMR, and the results are listed in Table 1.

From the results in Table 1 and Figure 7, an increasing amount of GMA decreases the molecular weight and increases the molecular weight distribution of the samples, therefore decreasing the melting point and recrystallization temperatures of the copolymers, as

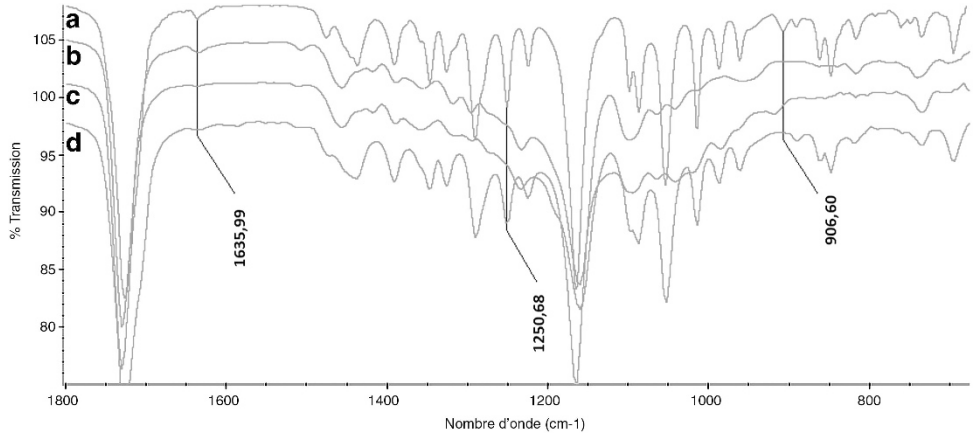

Figure 4 Fourier transform infrared spectroscopy spectra of the (**a**) monomer mixtures and of the products synthesized by catalysis of (**b**) TBD, (**c**) $Sn(Oct)_2$ and (**d**) 4-hydroxybenzenesulfonic acid. All copolymerizations were performed with [CL]/[catalyst]/[benzyl alcohol]/[hydroquinone] = 100/1/1/1 at 110 °C for 60 min. CL, caprolactone; $Sn(Oct)_2$, tin(II) bis(2-ethylhexanoate); TBD, 1,5,7-triazabicyclo[4.4.0]dec-5-ene. A full color version of this figure is available at *Polymer Journal* online.

Table 2 Conversion of CL and GMA from systems with different catalyst, all the copolymerizations were performed by [CL]:[GMA] = 5, [CL]:[cata.]:[benzyl alcohol]:[hydroquinone] = 100:1:1:1 at 110 °C for 60 min

Catalyst and amount	*Reaction time*	*Conversion of CL to repeat unit, by NMR, %*	*Conversion of GMA to repeat units, by NMR, %*	*Consumption of GMA double bonds, by NMR, %*
TBD, 1% of CL	60 min	100	76.95	0
4-HBSA, 1% of CL	120 min	46.62	44.13	93.10
$Sn(Oct)_2$, 1% of CL	120 min	100	24.58	51.86

Abbreviations: cata., catalyst; CL, caprolactone; GMA, glycidyl methacrylate; HBSA, hydroxybenzenesulfonic acid solution; NMR, nuclear magnetic resonance; $Sn(Oct)_2$, tin(II) bis(2-ethylhexanoate); TBD, 1,5,7-triazabicyclo[4.4.0]dec-5-ene.

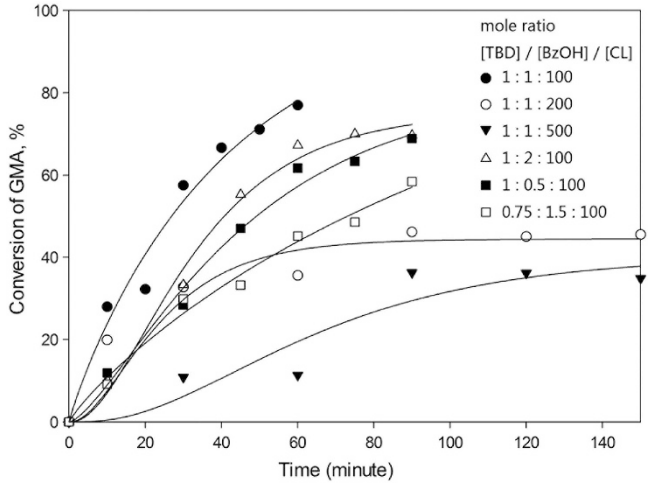

Figure 5 GMA conversion versus reaction time of CL-GMA copolymerization with different [TBD]/[benzyl alcohol] concentrations. All copolymerizations were performed with feeding ratio $[CL]_0/[GMA]_0 = 5/1$ at 110 °C. CL, caprolactone; GMA, glycidyl methacrylate; TBD, 1,5,7-triazabicyclo [4.4.0]dec-5-en.

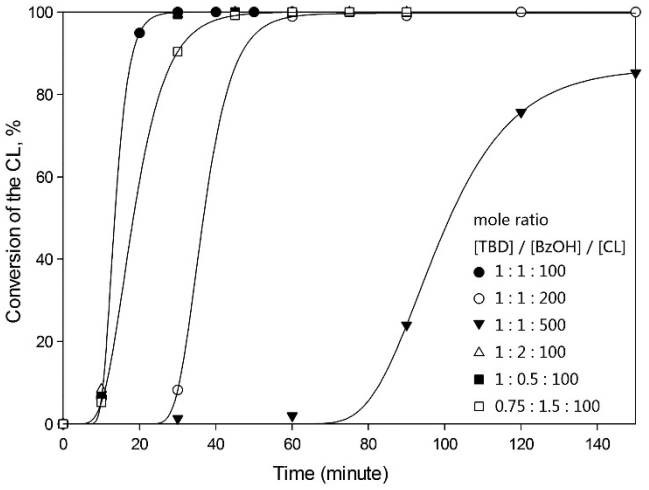

Figure 6 CL conversion versus reaction time of CL-GMA copolymerization with different [TBD]/[benzyl alcohol] concentrations. All copolymerizations were performed with feeding ratio $[CL]_0/[GMA]_0 = 5/1$ at 110 °C. CL, caprolactone; GMA, glycidyl methacrylate; TBD, 1,5,7-triazabicyclo [4.4.0]dec-5-en.

suggested by the differential scanning calorimetry results in Figures 8 and 9. Dual melting endotherms and recrystallization due to two different crystalline states of PCL segments are not observed for a feeding ratio of 2.5. This result can be explained by the different reactivities of GMA and CL. However, with a lower GMA content, caprolactone tends to homopolymerize and yields polymers with high molecular weights, whereas a higher GMA content results in an insoluble gel from double-bond polymerization cross-linking, even in the presence of the inhibitor.

Quantitative results are listed in Table 1. The sample with the feed ratio [GMA]/[CL] = 1/5 has the highest GMA conversion and moderate molar mass and therefore the highest functionality, which is suitable for copolymer synthesis.

Differential scanning calorimetry was used to characterize the thermal behavior of p(GMA-co-CL) synthesized with different monomer feeding ratios, and the results are shown in Figures 8 and 9. The glass transition temperature was estimated to be ~ -60

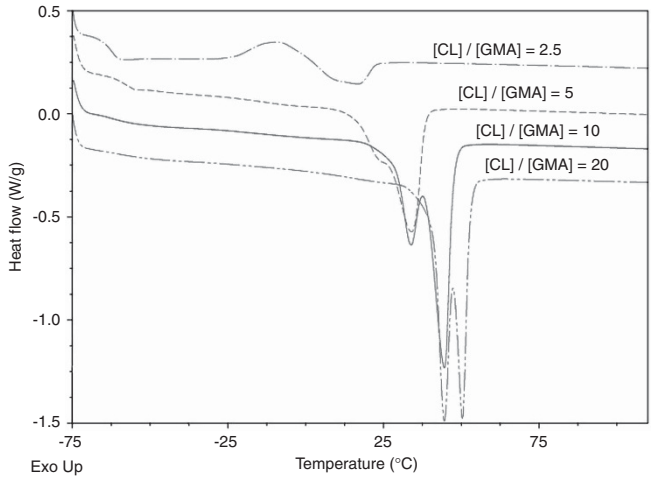

Figure 7 DSC thermographs of copolymers synthesized with different [CL]/[GMA] feeding ratios: recrystallization of the copolymer chains. All samples were obtained from copolymerization with parameters [CL]/[catalyst]/[benzyl alcohol]/[hydroquinone] = 100/1/1/1 at 110 °C for 60 min. CL, caprolactone; DSC, differential scanning calorimetry; GMA, glycidyl methacrylate. A full color version of this figure is available at *Polymer Journal* online.

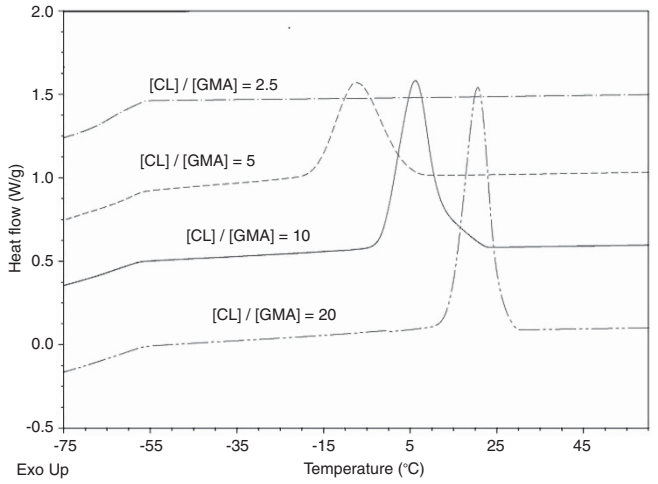

Figure 8 DSC thermographs of copolymers synthesized with different [CL]/[GMA] feeding ratios' melting transition of the copolymer chains. All samples were obtained from copolymerization with parameters [CL]/[catalyst]/[benzyl alcohol]/[hydroquinone] = 100/1/1/1 at 110 °C for 60 min. CL, caprolactone; DSC, differential scanning calorimetry; GMA, glycidyl methacrylate. A full color version of this figure is available at *Polymer Journal* online.

°C, corresponding to the caprolactone-rich phase. The products exhibit dual endotherms at 18.5 and 32.3 °C, corresponding to a melting–recrystallization–remelting sequence often observed in PCL.[36,37] These endotherms and the crystallization are shifted to lower temperatures with the incorporation of epoxy units into the PCL chains.[27]

Network formation using p(GMA-co-CL)

p(GMA-co-CL) with pendant methacrylate functions can be used to prepare novel networks. The use of a multi-mercapto reagent in the thiol–ene click reaction is expected to build networks by coupling p(GMA-co-CL) chains. Furthermore, p(GMA-co-CL) copolymerized with HEMA can also form networks in which p(GMA-co-CL) are expected to be linked by pHEMA chains that have molar mass distributions.

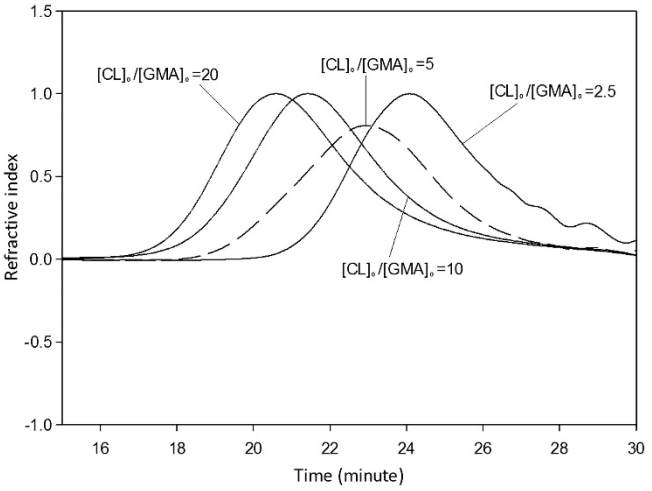

Figure 9 SEC graph of copolymers synthesized with different [CL]/[GMA] feeding ratios. All samples were obtained from copolymerization with parameters [CL]/[catalyst]/[benzyl alcohol]/[hydroquinone] = 100/1/1/1 at 110 °C for 60 min. CL, caprolactone; GMA, glycidyl methacrylate; SEC, size exclusion chromatography.

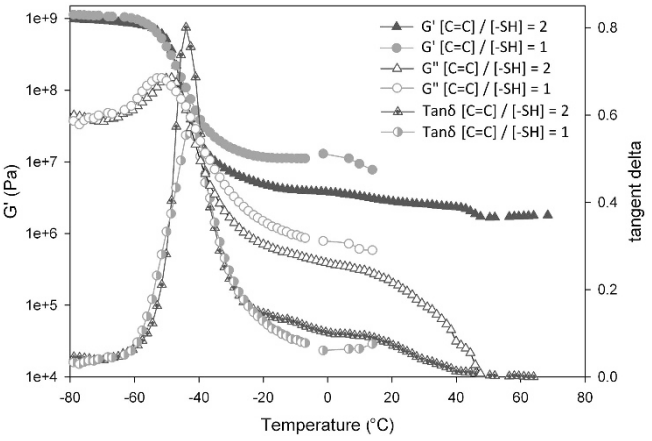

Figure 10 Storage moduli (G′), loss moduli (G″) and loss factors of the networks formed by p(GMA-co-CL) and trimethylolpropane tris (3-mercaptopropionate) with different mole ratios after UV irradiation. The p(GMA-co-CL) used is sample Run 3 in Table 1. Round spot curves: polymer with mole ratio [double bond]/[mercapto] = 1; triangle spot curves: polymer with mole ratio [double bond]/[mercapto] = 2. p(GMA-co-CL), poly(glycidyl methacrylate-co-caprolactone). A full color version of this figure is available at *Polymer Journal* online.

P(CL-co-GMA) network formation with multi-mercapto coupling agents. p(GMA-co-CL) was coupled with trimethylolpropane tris(3-mercaptopropionate) using different double bond/mercapto mole ratios to form networks via thiol–ene reaction through UV initiation. In this case, a photoinitiator was not necessary. Evaluation of the thermomechanical properties of the obtained products was performed using dynamic mechanical analysis. Figure 10 shows the moduli and loss tangent of cured samples with different [double bond]/[thiol] mole ratios.

These spectra indicate that networks were obtained because the storage moduli are higher than the loss moduli throughout the whole temperature range analyzed, and the appearance of a rubbery plateau is observed. Moreover, the narrow tanδ peak with its maximum value at $-40\,^{\circ}C$ indicates that a homogeneous PCL network was prepared. As expected, the network formed with the [double bond]/[thiol] mole ratio = 1 leads to a network with a higher storage modulus plateau and lower mass between crosslinks, M_c, than the case in which this ratio is 2.

Cross-linking of p(CL-co-GMA) and pHEMA. On the basis of previous results, p(GMA-co-CL) and HEMA copolymerization through UV initiation was studied. The effects of different reaction parameters (listed in Table 3) were analyzed.

[p(GMA-co-CL)]/[HEMA] mass ratio. The copolymerization of p(GMA-co-CL) (sample Run 3 in Table 1) and HEMA with different mass ratios was accomplished. Reactions were conducted until the complete consumption of double bonds was observed in Fourier transform infrared spectroscopy spectra, monitored by their absorption at $1630\,cm^{-1}$. Thermomechanical property evolution with temperature of these products is depicted in Figure 11.

Table 3 Syntheses parameters of p(CL-co-GMA)/poly 2-hydroxyethyl methacrylate/trimethylolpropane tris(3-mercaptopropionate) cooperated networks

Sample	*Feeding ratio of [p(GMA-co-CL)]: [HEMA], wt:wt*	*Tri-thiol amount introduced in networks, mol%*	*Functionality of p(GMA-co-CL) in network establishment*
Run 11	1.5/1	0	4.6
Run 12	1.25/1	0	4.6
Run 13	1/1	0	4.6
Run 14	1/2	0	4.6
Run 15	1.25/1	0	3.1
Run 16	1.25/1	0	1.3
Run 17	1.25/1	10	4.6
Run 18	1.25/1	20	4.6
Run 19	1.25/1	30	4.6
Run 20	1/1.5	10	4.6
Run 21	1/2	10	4.6

Abbreviations: HEMA, 2-hydroxyethyl methacrylate; p(CL-co-GMA), poly(caprolactone-co-glycidyl methacrylate).

Table 4 T_g and maximum tanδ of PHEMA and p(GMA-co-CL) phase in copolymers and their working area for damping

	p(GMA-co-CL) phase		*PHEMA phase*		
Samples	T_g, °C	$Tan\delta_{max}$	T_g, °C	$Tan\delta_{max}$	$\Delta tan\delta > 0.3$, °C
Run 11	16	0.29	68	0.28	—
Run 12	−38	0.10	60	0.44	30–117
Run 13	−49	0.19	74	0.42	34–97
Run 14	−55	0.04	84	0.48	53–108
Run 15	−28.1	0.12	53	0.52	23.0–73.7
Run 16	−32.5	0.14	71	0.50	32.1–90.4

Abbreviations: PHEMA, poly(2-hydroxyethyl methacrylate); p(GMA-co-CL), poly(glycidyl methacrylate-co-caprolactone); T_g, glass transition temperature.
The networks were synthesized without the introduction of thiols, Run 11—[p(GMA-co-CL)]:[HEMA] = 1.5:1—p(GMA-co-CL) $f = 4.6$; Run 12—1.25:1, $f = 4.6$; Run 13—1:1, $f = 4.6$, Run 14—1:2, $f = 4.6$; Run 15—1.25:1, $f = 3.1$; Run 16—1.25:1, $f = 1.3$.

G′ values greater than G″ throughout the temperature range confirm again the cross-linking of the products. For [p(GMA-co-CL)]/[HEMA] = 1/2 (Run 14), the pHEMA-rich phase is predominant and clear, with a distinct tanδ peak that is broadened at lower temperatures, whereas the glass transition temperature of the PCL-rich phase is almost undetectable. By reducing the quantity of HEMA ([p(GMA-co-CL)]/[HEMA] = 1/1, Run 13), two different tanδ peaks and an intermediate region with high tanδ are observed. Two different phases are separated out; the one at lower temperature corresponds to the PCL-rich phase, whereas the one at higher temperature corresponds to the pHEMA-rich phase. Two tanδ peaks shift toward each other (Table 4), indicating interactions with these two phases. The intermediate tanδ region indicates that several network structures are formed by linking PCL backbones with pHEMA segments that have different chain lengths. This structural evolution continues with [p(GMA-co-CL)]/[HEMA] = 1.25/1.

For [p(GMA-co-CL)]/[HEMA] = 1.5/1 (Run 11), the PCL- and pHEMA-rich phases are no longer distinguishable. A wide relaxation transition between the initial PCL- and pHEMA-rich phases is

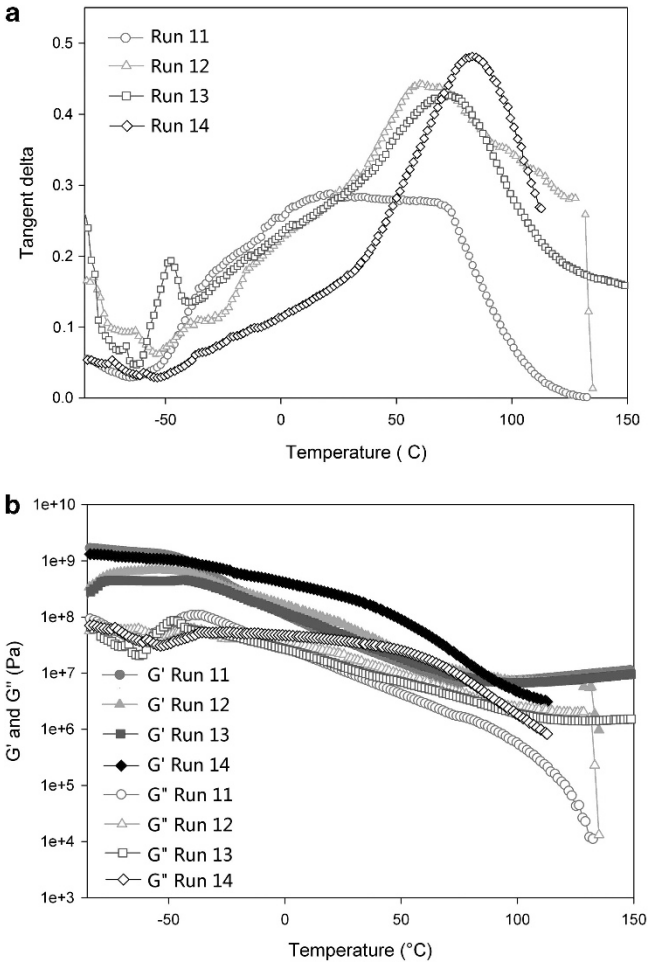

Figure 11 (**a**) Loss factor tanδ versus temperature of networks composed of different p(GMA-co-CL)/HEMA mass ratios. Run 11—[p(GMA-co-CL)]/[HEMA] = 1.5/1; Run 12—1.25/1; Run 13—1/1; Run 14—1/2. (**b**) Modulus G′ and G″ versus temperature of networks composed of different p(GMA-co-CL)/HEMA mass ratios. Run 11—[p(GMA-co-CL)]/[HEMA] = 1.5/1; Run 12—1.25/1; Run 13—1/1; Run 14—1/2. HEMA, 2-hydroxyethyl methacrylate; p(GMA-co-CL), poly(glycidyl methacrylate-co-caprolactone). A full color version of this figure is available at *Polymer Journal* online.

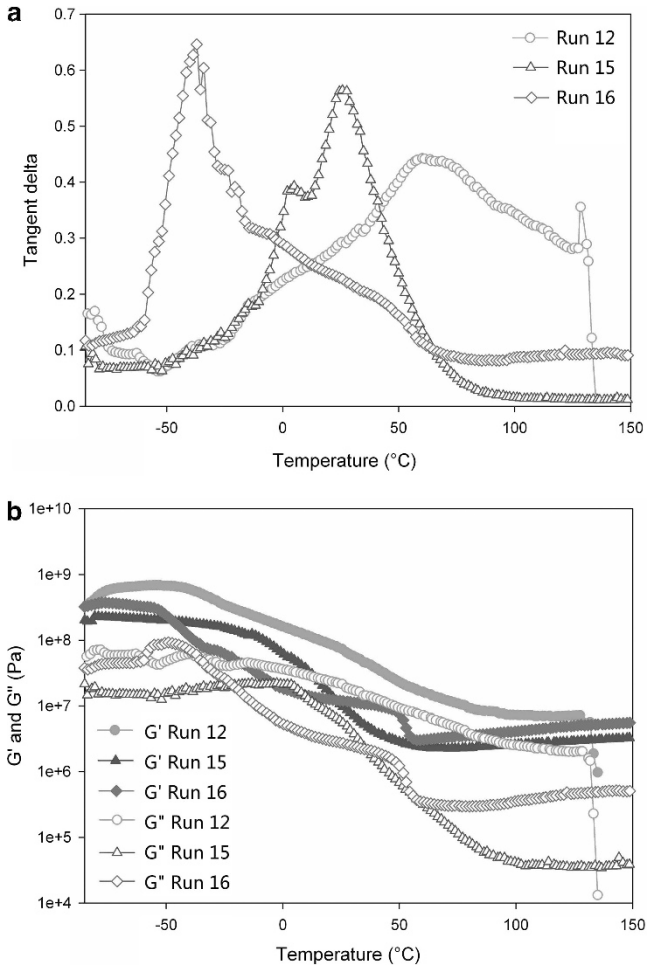

Figure 12 (**a**) Loss factor tanδ versus temperature of networks built of HEMA and p(GMA-co-CL) with different p(GMA-co-CL) functionalities. Mass ratio [copolymer]/[HEMA] = 1.25/1, Run 12—p(GMA-co-CL) $f = 4.6$; Run 13—$f = 3.1$; Run 14—$f = 1.3$. (**b**) Modulus G′ and G″ versus temperature of networks built of HEMA and p(GMA-co-CL) with different p(GMA-co-CL) functionalities. Mass ratio [copolymer]/[HEMA] = 1.25/1, Run 12—p(GMA-co-CL) $f = 4.6$; Run 13—$f = 3.1$; Run 14—$f = 1.3$. HEMA, 2-hydroxyethyl methacrylate; p(GMA-co-CL), poly(glycidyl methacrylate-co-caprolactone). A full color version of this figure is available at *Polymer Journal* online.

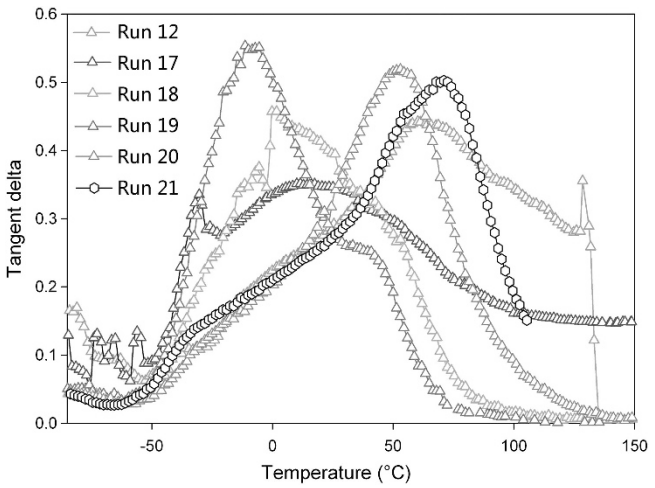

Figure 13 Loss factor tanδ versus temperature of networks synthesized with HEMA, p(GMA-co-CL) and thiol by different parameters. Run 12—[p(GMA-co-CL)]/[HEMA] = 1.25/1, without thiol; Run 17—1.25/1, 10% mol thiol; Run 18—1.25/1, 20% mol thiol; Run 19—1.25/1, 30% mol thiol; Run 20—1/1.5, 10% mol thiol; Run 21—1/2, 10% mol thiol. HEMA, 2-hydroxyethyl methacrylate; p(GMA-co-CL), poly(glycidyl methacrylate-co-caprolactone). A full color version of this figure is available at *Polymer Journal* online.

Table 5 T_g and tanδ peak values of GMA and CL phase in copolymers and their working areas for damping

	p(GMA-co-CL) phase		*PHEMA phase*		
Samples	T_g, °C	*Tan*δ_{max}	T_g, °C	*Tan*δ_{max}	*Δtanδ > 0.3, °C*
Run 12	−38	0.10	60	0.44	30 to 117
Run 17	−30.4	0.34	11.5	0.35	−34 to −29, −13 to 48
Run 18	1.6	0.45	42.6	0.32	−16 to 45
Run 19	−11.4	0.55	40.30	0.26	−31 to 23
Run 20	−28.1	0.12	53.0	0.52	−28
Run 21	−34.1	0.13	71.0	0.50	33 to 90

Abbreviations: PHEMA, poly(2-hydroxyethyl methacrylate); p(GMA-co-CL), poly(glycidyl methacrylate-co-caprolactone); T_g, glass transition temperature.
The networks were synthesized with the introduction of thiols. Run 12—[p(GMA-co-CL)]/[HEMA] = 1.25/1, without thiol; Run 17—1.25/1, 10% mol thiol; Run 18—1.25/1, 20% mol thiol; Run 19—1.25/1, 30% mol thiol; Run 20—1/1.5, 10% mol thiol; Run 21—1/2, 10% mol thiol.

obtained with a tanδ peak reduction. The tanδ curve is broadened and almost rectangular in a wide temperature zone. In these multi-component systems, the effective damping temperature range is broadened. All networks showed expanded damping peaks, with tanδ peak values above 0.3, as shown in Table 4.

Effects of p(CL-co-GMA) functionality on the p(CL-co-GMA)/HEMA network. p(GMA-co-CL) with different functionalities were copolymerized, each with the same amount of HEMA. The [p(CL-co-GMA)]/[HEMA] mass ratio was held at 1.25. The DMA results of the obtained samples are illustrated in Figure 12.

For the network built with p(GMA-co-CL) that had lower functionality ($f = 1.3$, Run 16), a tanδ peak is obtained at lower temperature. This peak is attributed to p(GMA-co-CL) segments with lower GMA quantities (−60 to −15 °C). The copolymerization of these p(GMA-co-CL) with HEMA is relatively lower. In this network, p(GMA-co-CL) copolymerized with HEMA can be observed with broadened tanδ peaks at higher temperatures, with damping effects ranging from −15 to 60 °C.

The network built with highly functionalized p(GMA-co-CL) ($f = 4.6$, Run 12) shows the reverse effect. The more functionalized p(GMA-co-CL) is mostly cross-linked and modified, yielding a network exhibiting relaxations similar to those of pHEMA. The less functionalized part is the less modified part and leads to networks having glass transitions at lower temperatures. A particular damping effect between −15 and 140 °C is obtained.

For the network built using intermediate p(GMA-co-CL) functionalization ($f = 3.1$, Run 15), two transitions are observed. The tanδ corresponding to the PCL- and pHEMA-rich phases shift toward each other, revealing an important compatibility effect. These peaks become relatively high and narrow, indicating increasing mobility in the region of relaxation transition (0–60 °C).

Effects of the addition of multi-thiols on the p(CL-co-GMA)/HEMA network. Multi-thiols act not only as cross-linkers but also as efficient chain transfer agents during radical polymerizations that

can directly affect the polymerization degree of the polymer.[38,39] Meanwhile, multi-thiols also reduce oxygen inhibition during radical photopolymerizations.[40] In this study, tri-thiols were added during p(CL-co-GMA)/HEMA copolymerization. Figure 13 plots loss factors (tanδ) versus temperature for networks obtained with different multi-thiol contents.

Three cases should be considered, according to the number of mercapto groups that react per tri-thiol molecule. For the first case, only one mercapto group reacts. The interruption of pHEMA chain growth results in a pendant pHEMA segment with two ending mercapto groups on p(GMA-co-CL) chain, which is equivalent to the loss of a methacrylate function on the PCL backbone that will not participate in the formation of bridges between p(GMA-co-CL) chains. For the second case, two mercapto groups react, which results in the growth of pHEMA chains being maintained, leading to a segment connecting two chains and bearing one residual mercapto group. For the last case, all mercapto groups react, resulting in an additional cross-linking point. The three cases actually occur in parallel, with a predominance of a particular case depending on the stoichiometry of the various reagents.

For all experiments, networks were obtained (G' higher than G'' for all temperature ranges). The shape of the tanδ curve corresponding to Run 12 is only maintained for Run 21. In this case, the addition of thiol is compensated by the addition of significant quantities of HEMA. When the quantity of HEMA is lower, a small shift of tanδ toward lower temperatures is obtained for Run 20 and much more significant for Run 17.

As expected, the addition of thiols to Run 12 results in an effect equivalent to the decrease of p(GMA-co-CL) functionality, especially when the thiol amount is increased, as shown by Runs 17–19. These results can be explained by a transfer reaction leading to pendant chains with residual mercapto groups. When the quantities of mercaptans increased in runs 18 and 19, this effect was enhanced. The damping properties of these networks are shown in Table 5.

CONCLUSION

An efficient and easy synthetic route for methacrylated PCL through the ring-opening copolymerization of GMA and caprolactone is proposed. The molar mass and functionality of these p(GMA-co-CL) copolymers can be altered by changing the reaction parameters, such as the nature and ratio of catalyst and co-initiator or monomer stoichiometry. The obtained copolymers can be directed by thiol–ene reactions with trimethylolpropane tris(3-mercaptopropionate) to form homogeneous transparent networks. When p(GMA-co-CL) copolymerizes with HEMA, the obtained network has original and tunable damping properties that can be adapted by changing curing parameters such as monomer ratios and functionalities. Furthermore, the addition of multi-thiols can lead to networks with supplementary cross-linking points.

ACKNOWLEDGEMENTS

We are grateful for the financial support from the China Scholarship Council (state scholarship fund). This work benefited from the international cooperation between the Université Jean-Monnet, Saint-Etienne (France), and the East China University of Science and Technology (China).

1 Trakulsujaritchok, T. & Hourston, D. Damping characteristics and mechanical properties of silica filled PUR/PEMA simultaneous interpenetrating polymer networks. *Eur. Polym. J.* **42,** 2968–2976 (2006).
2 Babkina, N., Lipatov, Y. S. & Alekseeva, T. Damping properties of composites based on interpenetrating polymer networks formed in the presence of compatibilizing additives. *Mech. Compos. Mater.* **42,** 385–392 (2006).
3 Tang, D., Zhang, J., Zhou, D. & Zhao, L. Influence of BaTiO3 on damping and dielectric properties of filled polyurethane/unsaturated polyester resin interpenetrating polymer networks. *J. Mater. Sci.* **40,** 3339–3345 (2005).
4 Fu, W. & Chung, D. (Brief Communication) Vibration reduction ability of polymers, particularly polymethylmethacrylate and polytetrafluoroethylene. *Polym. Polym. Compos.* **9,** 423–426 (2001).
5 Chung, D. Review: materials for vibration damping. *J. Mater. Sci.* **36,** 5733–5737 (2001).
6 Corsaro, R. D. & Sperling, L. H. Sound and Vibration Damping with Polymers, vol. 424. ACS Publications: 1990.
7 Albertsson, A. C. & Varma, I. K. Recent developments in ring opening polymerization of lactones for biomedical applications. *Biomacromolecules* **4,** 1466–1486 (2003).
8 Jerome, C. & Lecomte, P. Recent advances in the synthesis of aliphatic polyesters by ring-opening polymerization. *Adv. Drug Deliv. Rev.* **60,** 1056–1076 (2008).
9 Okada, M. Chemical syntheses of biodegradable polymers. *Prog. Polym. Sci.* **27,** 87–133 (2002).
10 Yeh, C. C., Chen, C. N., Li, Y. T., Chang, C. W., Cheng, M. Y. & Chang, H. I. The effect of polymer molecular weight and UV radiation on physical properties and bioactivities of PCL films. *Cell Polym.* **30,** 261–276 (2011).
11 Tay, B. Y., Zhang, S. X., Myint, M. H., Ng, F. L., Chandrasekaran, M. & Tan, L. K. A. Processing of polycaprolactone porous structure for scaffold development. *J. Mater. Process Tech.* **182,** 117–121 (2007).
12 Baji, A., Wong, S. C., Srivatsan, T. S., Njus, G. O. & Mathur, G. Processing methodologies for polycaprolactone-hydroxyapatite composites: a review. *Mater. Manuf. Process.* **21,** 211–218 (2006).
13 Yoshimoto, H., Shin, Y. M., Terai, H. & Vacanti, J. P. A biodegradable nanofiber scaffold by electrospinning and its potential for bone tissue engineering. *Biomaterials* **24,** 2077–2082 (2003).
14 Diba, M., Kharaziha, M., Fathi, M. H., Gholipourmalekabadi, M. & Samadikuchaksaraei, A. Preparation and characterization of polycaprolactone/forsterite nanocomposite porous scaffolds designed for bone tissue regeneration. *Compos. Sci. Technol.* **72,** 716–723 (2012).
15 Rai, B., Teoh, S. H., Hutmacher, D. W., Cao, T. & Ho, K. H. Novel PCL-based honeycomb scaffolds as drug delivery systems for rhBMP-2. *Biomaterials* **26,** 3739–3748 (2005).
16 Ebersole, G. C., Buettmann, E. G., MacEwan, M. R., Tang, M. E., Frisella, M. M., Matthews, B. D. & Deeken, C. R. Development of novel electrospun absorbable polycaprolactone (PCL) scaffolds for hernia repair applications. *Surg. Endosc.* **26,** 2717–2728 (2012).
17 Zhu, Y. B., Gao, C. Y. & Shen, J. C. Surface modification of polycaprolactone with poly(methacrylic acid) and gelatin covalent immobilization for promoting its cytocompatibility. *Biomaterials* **23,** 4889–4895 (2002).
18 Riva, R., Lenoir, S., Jerome, R. & Lecomte, P. Functionalization of poly(epsilon-caprolactone) by pendant hydroxyl, carboxylic acid and epoxide groups by atom transfer radical addition. *Polymer* **46,** 8511–8518 (2005).
19 Coudray, S., Pascault, J. & Taha, M. Acrylated polyurethanes by reactive extrusion. *Polym. Bull.* **32,** 605–610 (1994).
20 Mallek, H., Jegat, C., Mignard, N., Abid, M., Abid, S. & Taha, M. One-step synthesis of PCL-urethane networks using a crosslinking/de-crosslinking agent. *J. Polym. Sci. A Polym. Chem.* **50,** 728–737 (2013).
21 Mecerreyes, D., Humes, J., Miller, R. D., Hedrick, J. L., Detrembleur, C., Lecomte, P., Jérôme, R. & San Roman, J. First example of an unsymmetrical difunctional monomer polymerizable by two living/controlled methods. *Macromol. Rapid Commun.* **21,** 779–784 (2000).
22 Mecerreyes, D., Miller, R. D., Hedrick, J. L., Detrembleur, C. & Jerome, R. Ring-opening polymerization of 6-hydroxynon-8-enoic acid lactone: novel biodegradable copolymers containing allyl pendent groups. *J. Polym. Sci. A Polym. Chem.* **38,** 870–875 (2000).
23 Ahmetli, G., Kocak, A. & Yazicigil, Z. Kinetics of the copolymerization of alkylene oxides with glycidyl methacrylate. *J. Appl. Polym. Sci.* **106,** 3710–3715 (2007).
24 Bicak, N. & Karagoz, B. Synthesis of new polyesters with methacrylate pendant groups. *Polym. Bull.* **56,** 87–93 (2006).
25 Fernandez, X., Salla, J. M., Serra, A., Mantecon, A. & Ramis, X. Cationic copolymerization with a spirobislactone with of cycloaliphatic epoxy resin lanthanum triflate as initiator: I. Characterization and shrinkage. *J. Polym. Sci. A Polym. Chem.* **43,** 3421–3432 (2005).
26 Labbe, A., Brocas, A. L., Ibarboure, E., Ishizone, T., Hirao, A., Deffieux, A. & Carlotti, S. Selective ring-opening polymerization of glycidyl methacrylate: toward the synthesis of cross-linked (Co)polyethers with thermoresponsive properties. *Macromolecules* **44,** 6356–6364 (2011).
27 Bednarek, M. & Kubisa, P. Copolymerization with the feeding of one of the comonomers: cationic activated monomer copolymerization of epsilon-caprolactone with ethylene oxide. *J. Polym. Sci. A Polym. Chem.* **43,** 3788–3796 (2005).
28 Uenishi, K., Sudo, A. & Endo, T. Anionic alternating copolymerization behavior of bifunctional six-membered lactone and glycidyl phenyl ether. *J. Polym. Sci. A Polym. Chem.* **47,** 3662–3668 (2009).
29 Sadik, T., Massardier, V., Becquart, F. & Taha, M. Synthesis and characterizations of poly (ethylene-co-vinylalcohol)-grafted-poly (3-hydroxybutyrate-co-hydroxyvalerate) copolymers. *Polymer* **53,** 4585–4594 (2012).

30 Odian, G. Ring-opening Polymerization. in Principles of Polymerization. 4th edn. (Wiley & Sons, Inc., Hoboken, NJ, USA, 2004).
31 Bouyahyi, M., Pepels, M. P. F., Heise, A. & Duchateau, R. Omega-pentandecalactone polymerization and omega-pentadecalactone/epsilon-caprolactone copolymerization reactions using organic catalysts. *Macromolecules* **45,** 3356–3366 (2012).
32 Nikolic, G., Zlatkovic, S., Cakic, M., Cakic, S., Lacnjevac, C. & Rajic, Z. Fast Fourier transform IR characterization of epoxy GY systems crosslinked with aliphatic and cycloaliphatic EH polyamine adducts. *Sensors* **10,** 684–696 (2010).
33 Chung, K., Takata, T. & Endo, T. Anionic cross-linking of polymers having an epoxy group in the side chain with bicyclic and spirocyclic bis (γ-lactone) s. *Macromolecules* **30,** 2532–2538 (1997).
34 Sato, T., Oki, T., Seno, M. & Hirano, T. Radical and cationic polymerizations of 3-ethyl-3-methacryloyloxymethyloxetane. *J. Polym. Sci. A Polym. Chem.* **39,** 1269–1279 (2001).
35 Simon, L. & Goodman, J. M. The mechanism of TBD-catalyzed ring-opening polymerization of cyclic esters. *J. Org. Chem.* **72,** 9656–9662 (2007).
36 Meng, Y. F., Li, H. F., Wen, H. Y., Jiang, S. C. & An, L. J. Study on crystallization of poly(ε-caprolactone) in poly(ε-caprolactone)/poly(vinyl methyl ether) blends. *Acta Polym. Sin.* **2,** 198–202 (2007).
37 Lezcano, E. G., Coll, C. S. & Prolongo, M. G. Melting behaviour and miscibility of poly(epsilon-caprolactone) plus poly(4-hydroxystyrene) blends. *Polymer* **37,** 3603–3609 (1996).
38 Boutevin, B., Snoussi, M. H. & Taha, M. Radical telomerization of glycidyl methacrylate with benzene thiol & dodecane thiol. *Eur. Polym. J.* **21,** 445–447 (1985).
39 Boutevin, B., Mouanda, J., Pietrasanta, Y. & Taha, M. Synthesis of block cotelomers involving a perfluorinated chain and a hydrophilic chain. II. Use of fluorinated telogens with iodine or thiol end groups. *J. Polym. Sci. A Polym. Chem.* **24,** 2891–2902 (1986).
40 Shin, J., Nazarenko, S. & Hoyle, C. E. Effects of chemical modification of thiol-ene networks on enthalpy relaxation. *Macromolecules* **42,** 6549–6557 (2009).